Photoelectrochemical System Studies

A. Bansal, O. Khaselev and J. A. Turner
National Renewable Energy Laboratory
1617 Cole Boulevard, Golden, Colorado 80401

ABSTRACT

The efficiency for any solar-to-hydrogen conversion process is particularly important because an area of land must be covered to collect the sunlight. Any efficiency losses in the system must be made up by an increase in the collector area. This will ultimately have a significant impact on the overall cost and siting ability of such a system. Section one of this report will explore the efficiency gains from a direct conversion system as compared to a separated PV/electrolysis system. Section two will discuss our results looking at the catalysis of hydrogen production on semiconductor electrodes.

EFFICIENCY OF PEC SYSTEMS

The energy efficiency of electrolysis can generally be defined as the chemical potential of hydrogen divided by the voltage required for electrolysis operation [1]. At the normal operating current density of commercial electrolyzers (~1 A/cm^2), this voltage ranges from 1.8—2.0 volts. Thus, an electrolyzer operating at 1.9 volts operates with an energy efficiency of 65% (1.23/1.9). Combining this electrolysis efficiency with a 12% PV array efficiency gives a solar-to-hydrogen efficiency of 7.8%. To increase the overall solar-to-hydrogen efficiency, the energy efficiency of electrolysis must be increased; thus, one must operate at a lower voltage. This requires better catalysts (particularly on the oxygen side), or a decrease in the current density (which results in a decrease in the rate of hydrogen production). Maintaining the rate of hydrogen production while reducing the current density could be done by increasing the area of the electrodes (or adding more electrolyzers), but costs would increase due to an increase in the amount of material used for the electrolyzer.

A photoelectrochemical (PEC) system combines the harvesting of solar energy with the electrolysis of water [2]. Depending on the type of semiconductor material and the solar intensity, the current density for electrolysis with a PEC system is 10-30 mA/cm^2. Figure 1 presents a current-voltage curve for water splitting in an electrochemical cell consisting of two Pt electrodes of identical area. At a current density similar to short-circuit photocurrent from a solar cell, hydrogen and oxygen generation is achieved at an effective applied voltage of approximately 1.35 V, giving rise to an electrolysis efficiency of 91% [3]. One of the major advantages then of a direct conversion photoelectrochemical system is that the area available for electrolysis approximates that of the solar cell. A PEC hydrogen generation system not only eliminates most of the costs of the electrolyzer, but it also has the possibility of increasing the overall efficiency of the process leading to a further decrease in costs. Note, although this experiment was done with Pt electrodes, at this current density, less expensive nickel and metal oxide electrodes could be used with similar results.

We have previously shown a high solar-to-hydrogen PEC conversion device [4], but problems of semiconductor stability, and interfacial kinetics, make it difficult to quantify the efficiency gains from such a PEC system. For this work, we used an integrated PV/electrolysis design to emulate a PEC system. Unlike a direct-conversion PEC system, an integrated PV/electrolysis system has separated PV and electrolyzer parts. However, for an integrated system, the area of the electrolyzer system is identical to the area of the PV collector. These integrated systems allow us to study the issues involving the effects of current density, solar intensity variability, and light concentration on the overall efficiency for hydrogen production. In this study, we utilized an integrated PV/electrolysis design based on a low-cost amorphous silicon (a-Si). multijunction device. This cell is capable of generating a voltage sufficient for water splitting, and we note that its lower system cost, combined with the good efficiency, represents an important area of research for integrated hydrogen production systems. It is demonstrated that this monolithic PV/electrolysis configuration can lead to a higher solar-to-hydrogen conversion efficiency than coupled systems involving electrolyzers and photovoltaic solar cells alone.

For an integrated PV/electrolysis configuration to work properly, the solar cell must provide sufficient voltage to drive the water redox reactions, and also provide any additional voltage needed to overcome the overvoltage losses resulting from the hydrogen and oxygen evolution reactions. The total output photovoltage must include the thermodynamics for water splitting (1.23 volts at 25°C), polarization losses η_a and η_c, for the anodic and cathodic processes respectively, and the IR potential drop in the bulk of electrolyte, which can be significant when gas evolution occurs. A multijunction integrated PV/electrolysis configuration comprises either a tandem (or triple) pn-pn/metal/electrolyte cell, with water reduction occurring at the back-contact/electrolyte interface, and oxidation occurring at the electrolyte/counter electrode (anode) interface, or alternately, a tandem np-np/metal/electrolyte cell with water oxidation occurring at the back-contact/electrolyte interface and reduction occurring at the electrolyte/counter electrode (cathode) interface. Figure 2 shows the power curve for the triple junction p-i-n a-Si solar cell under 100 mW/cm^2 illumination, clearly indicating its ability to provide sufficient voltage for water splitting. Figure 3 shows the bias-voltage dependence of the photocurrent (hydrogen production) for a triple-junction a-Si(Pt)/2**M** KOH/Pt cell. The bias-voltage characteristics are consistent with that expected from the current-voltage characteristics shown in Figures 1 and 2. For the triple-junction a-Si(Pt)/2**M** KOH/Pt cells, the light-limited current was reached approximately at zero bias. Operated at zero bias, with shorted electrodes, the cell generated hydrogen and oxygen.

In operation, an ideal integrated PV/electrolysis system would operate under short-circuit conditions. For such configuration, the efficiency for hydrogen production can be calculated using the equation: efficiency = (power out)/(power in). The input power is the incident light intensity of 100 mW/cm^2. For the output power, assuming 100% photocurrent electrolysis efficiency, the hydrogen production photocurrent is multiplied by 1.23 volts, the ideal fuel cell limit at 25 °C (lower heating value [LHV] of hydrogen). Using this calculatation, our experimental results for the hydrogen production efficiency for the triple junction a-Si(Pt)/2M KOH/Pt it is:

$$1.23V \bullet 6.4mA/cm^2/100mW/cm^2 = 7.8\%.$$

The value for the a-Si system is significant in that this efficiency is realized by a PV cell with only a 9% solar-to-electrical efficiency. Because of the lower current density, this system is performing water electrolysis with an equivalent efficiency of 86% (effective electrolysis voltage of 1.42 volts [LHV]). This means that the maximum operating voltage of the a-Si PV cell is close to that required for electrolysis.

To maximize solar-to-hydrogen efficiency of the PV/electrolysis system operating at short circuit condition, a multijunction photovoltaic cell should be specifically designed to match electrical parameters for water splitting. For any direct solar-to-hydrogen conversion system, the maximum voltage that can be used in an efficiency calculation is fixed by the chemical potential of hydrogen. In order to increase the conversion efficiency, the current (and therefore the rate of production of hydrogen) must be increased. The ideal system would reach maximum power at less than 1.6 V, and a current density more than 20 mA/cm^2. Although the solar-to-electrical conversion efficiency of such cell would be less, the solar-to-hydrogen efficiency of the integrated PV/electrolysis system (and an analogous PEC system) would benefit.

CATALYSIS FOR THE PHOTOELECTROCHEMICAL PRODUCTION OF HYDROGEN

For a practical, stable and efficient semiconductor based water splitting system, four criteria must be simultaneously satisfied. The bandgap of the semiconductor must be greater than 1.7 eV, the band edges of the semiconductor must overlap the H_2/H_2O and O_2/H_2O redox potentials *under H_2/O_2 evolution condition* and charge transfer across the semiconductor-liquid interface should be fast (Fig. 4). In addition, the semiconductor surface should be chemically stable in the aqueous media.

Although p-type GaInP$_2$ with a bandgap of 1.8-1.9 eV has been identified as a promising photocathode for water splitting, its band edges are 0.2-0.4 V too negative to effect photoelectrolysis.[5-7] Electrochemical investigations of GaInP$_2$ in aqueous media have found that the semiconductor surface is unstable and susceptible to corrosion [8]. Furthermore, it is not known if the charge transfer rate from p-GaInP$_2$ to water under illumination is sufficiently high or if this rate can be further catalyzed.

At present, there is no information on the energetic position of the band edges or on the kinetics of charge transfer at the p-GaInP$_2$/water interface under illumination i.e. under conditions of H$_2$ evolution. Several impedance measurements in the literature have previously reported that band edges of semiconductors are not fixed and are prone to migration under illumination [9-19]. These changes in flatband potential under illumination have been interpreted to indicate evidence of surface effects such as charge trapping, adsorption or changes in the surface chemistry. The band edge positions are also known to be strongly affected by interfacial kinetics under illumination [13,15]. Increased band edge migration as a result of illumination has been observed for interfaces with poor interfacial charge transfer ability and this migration has been suppressed by treating the semiconductor surfaces with transition metal catalysts [14,20].

In this report, we describe our work on evaluating the effect of interfacial kinetics on the band edge positions of the p-GaInP$_2$/water interface under illumination i.e. under conditions of H$_2$ evolution. In addition, we describe the results of C-V and I-V measurements on p-GaInP$_2$ surfaces modified with transition metal ions to evaluate their effectiveness as reagents for inducing band edge shifts in the dark and as electrocatalysts for suppressing band edge migration under illumination. In this study, the flow of photogenerated cathodic current at the semiconductor surface under illumination corresponds to generation of hydrogen from photoelectrolysis of water.

Note: A semiconductor surface treatment such as the adsorption of a transition metal ion, can have two distinct effects on the energetics of the interface. Due to change of net charge in the Helmholtz layer, adsorption of a transition metal as a charged species (ion) on the

semiconductor surface can change the band edge position relative to the band edge position for an underivatized surface - *in the dark.* This effect is referred to as band edge "shift" or flatband "shift" in this paper. On the other hand, the measured band edge position vs. a solution reference can also move as a result of illumination due to accumulation of photogenerated charges at the interface. This movement is not due to a change in the charge in the Helmholtz region. Its extent is determined by the level of illumination at the semiconductor surface and the interfacial charge transfer kinetics. This movement can be suppressed if the transition metal species acts as an electrocatalyst and catalyses charge transfer across the interface, thereby reducing the accumulation of charge at the interface. In this report, the movement of band edges due to photoelectron accumulation is referred to as "migration". In measuring the "migration" effect, the band edge position of a surface under a given level of illumination is compared with the band edge position for *the same surface* in the dark. Although both of these effects have been individually described in the literature as "shifts" of band edges, [9-19] we have used the terms "shift" and "migration" in this paper to distinguish between the two.

Impedance Data Analysis - A detailed impedance analysis of the p-GaInP$_2$/water system in the dark has been previously reported, in which capacitance data in the frequency range 500 < f < 10^5 Hz, was attributed to the space charge layer of the semiconductor [7]. For the purpose of this study the series RC circuit (Scheme I) where R_S is the series resistance of the circuit and C_{SC} is the capacitance of the space charge region, was deemed as the simplest circuit that could adequately describe the trends in the movement of the flatband potential under illumination [21]. The slope and x-axis intercept of the Mott-Schottky plots were used to determine dopant density and the flatband potentials respectively.

Scheme I

Flatband potentials of etched p-GaInP$_2$/water interfaces - Figure 5 shows representative Mott-Schottky plots for etched p-GaInP$_2$ electrodes immersed in 0.20 M K$_2$SO$_4$ solutions of pH 1, 7 and 13. Data collected at each pH in the dark and compared to that under illumination show a negative migration of the flatband potential with increasing levels of light intensity. Figure 6a shows the corresponding flatband potentials calculated from similar Mott-Schottky plots for five different pH values, and the associated shifts from increased illumination. The curves for pH 1 and 13 were measured in unbuffered solutions of 0.20 M K$_2$SO$_4$, which were made acidic or basic using the necessary amount of H$_2$SO$_4$ or KOH, respectively. The curves for pH 4, 7 and 10 were measured in commercial phthalate (pH 4), phosphate (pH 7) and carbonate (pH 10) buffer solutions.

Figure 6b shows the same data as the net migration of the flatband potentials measured vs. the values observed in the dark. It is seen that even at low levels of illumination e.g. ~0.1 mA/cm2, the GaInP$_2$ flatband potentials (band edges) move up to 0.3 V negative as compared to their positions in the dark. As the level of illumination is increased the negative migration of the band edges becomes more pronounced with values reaching almost one volt for some pHs at current densities of around 10 mA/cm^2.

Effect of transition-metal ions on the flatband potential of p-GaInP$_2$/water interface under illumination - Figure 7 shows Mott-Schottky plots for an untreated and a Ru[III]-treated p- GaInP$_2$ surface, measured in the dark and under increasing illumination intensity in 3 M KOH solution. Figure 8a shows the corresponding flatband potentials calculated from similar Mott-Schottky plots of etched and metal-ion treated p- GaInP$_2$ electrodes in the 3 M KOH solution. In addition, the figure also shows flatband potentials measured with a GaInP$_2$ electrode modified with electrodeposited platinum. Figure 8b shows the same data plotted as the migration of the flatband potentials measured vs. the values observed in the dark. While the etched only (untreated) surface exhibits significant migration of the flatband potential under illumination, the migration is significantly suppressed for the metal-ion treated surfaces, with the RuIII treated electrode showing the best overall behavior. Table I lists the flatband potentials (V_{fb}) observed for the underivatized and the metal-ion treated surfaces in the dark and under illumination. The 'light' data reported corresponds to a current density of 0.7-1.0 mA/cm^2.

Effect of transition-metal ions on the I-V properties of p- GaInP$_2$/water interface - Figure 9 shows the effect of metal-ion treatment on the current-voltage properties of the untreated (etched only) and metal-ion treated p-GaInP$_2$ electrodes in 3 M KOH solution. The metal-ion treated surfaces exhibit improved fill factors and decreased hysteresis as compared to the untreated surface. The open circuit voltages (Voc) observed for the metal-ion treated surfaces were generally more positive than the untreated surface. The Voc values observed for the underivatized and the metal-ion treated surfaces for the positive are also given in Table I.

A practical single semiconductor photoelectrochemical system for water splitting requires that the three conditions of bandgap, band edge overlap and fast kinetics must be simultaneously satisfied (Fig. 4). The first two conditions are determined, respectively, by the energetics of the semiconductor and the semiconductor/liquid junction, while the third condition is determined by the kinetics of the reaction of interest at the interface. In the present case, the reaction of interest is generation of hydrogen from photoelectrolysis of water. From the above description it would seem that in a p-type semiconductor/liquid junction cell, the first two conditions would be the only necessary and sufficient conditions for H$_2$ evolution at the semiconductor interface. However, we have shown here that fast interfacial kinetics is also a necessary condition for any significant amount of hydrogen evolution. The kinetics of interfacial charge transfer strongly affects the energetics of a semiconductor/liquid junction. Furthermore, we have shown (as also have others [7-15,18-20] that it is erroneous to assume that the band edge positions of the semiconductors remain in the same position during current flow under illumination as in the dark, except perhaps for interfaces with extremely fast interfacial charge transfer rates. This realization is significant for GaInP$_2$ because it implies that any surface modification that is applied to shift semiconductor band edges to achieve band edge overlap must also not compromise interfacial kinetics or else any band edge shifts could be nullified by band edge migration under illumination [6,7].

The nature and amount of the catalyst at a semiconductor/electrolyte interface is very important in determining the activity of the electrocatalyst. The coverage should be high enough to affect a high rate of hydrogen production and yet should not be so high as to impede light absorption by the semiconductor. Although the exact nature and the amount of the transition metal species adsorbed on the p-GaInP$_2$ surface is presently unknown, a previous study on a similar substrate (GaAs) suggests that the metal ions may be deposited as complexes, in submonolayer to a few monolayers amounts, via a redox reaction with the surface semiconductor atoms [22]. In any case, the lack of flatband shifts in the dark upon metal-ion treatment suggests that the metal complexes are present as overall neutral species on the GaInP$_2$ surface. If precious metals are to be used as catalysts for photoelectrochemical hydrogen evolution, it is important that the

absolute minimum amount required for the highest catalysis be determined. Although the amount of catalyst deposited on the semiconductor surface has not been controlled or optimized in this study, it is clear that significant catalysis can be obtained even with near monolayer amounts of transition metal ions.

CONCLUSIONS

This work shows that the p-GaInP$_2$ band edges migrate negative under illumination in solutions with pH ranging from 1-14.5. The displacement is not due to a change in the pH of the semiconductor microenvironment but is caused by the accumulation of photogenerated electrons at the interface due to poor interfacial charge transfer kinetics. Differentiating between the two is important for developing appropriate surface modification strategies to realize an effective water-photoelectrolysis system. From the experiments described above, it becomes imperative that any surface modification scheme used to achieve the 'band edge overlap condition' must not compromise the charge transfer kinetics at the interface. Our observations indicate a less than optimal rate of charge transfer across the p-GaInP$_2$/water interface and underscore the necessity of catalysis at the p-GaInP$_2$/water interface.

Treatment with transition-metal ions is found to effectively electrocatalyse transfer of photogenerated electrons from the semiconductor to the liquid and to arrest the undesired band edge migration under illumination. p-GaInP$_2$ electrodes treated with Ru^{III}, Rh^{III}, Co^{III} and Os^{III} ions exhibit improved fill factors and small positive increases in the Voc. Light limited current levels are reached at lower applied voltages. Ru^{III} and Rh^{III} treatments are found to suppress band edge migration better than electrochemically deposited platinum treatment that is widely used as a hydrogen evolution catalyst in the literature. The observation that even the best catalysts of this study (Ru^{III} and Rh^{III}) show ~0.25 V band edge migration at a current density of ~10 mA/cm^2 suggests that other catalysts can be identified which can support higher currents through the interface without causing appreciable band edge migration.

Although the metal-ion treatment does not shift the band edges of p-GaInP$_2$ positive enough to affect unassisted photoelectrolysis, nevertheless, it can be applied to tandem cell designs where it can reduce the voltage assistance required by the p-GaInP2 top layer to split water, thereby increasing the efficiency (by decreasing the energy input required) of photo-driven hydrogen production [4].

FOOTNOTES AND REFERENCES

[1] *Energy efficiencies can really only be defined as power out/power in. In this case, we are assuming an ideal fuel cell running at the same current density as the electrolyzer.*
[2] A. J. Bard and M. A. Fox, *Acc. Chem. Res.* 1995; **28**:141.
[3] *Note that 1.35 volts is less than the thermodynamic potential required to split water. The additional energy needed for the reaction comes from the surrounding environment as heat. If one were to run a continuous electrolysis at 1.35 volts, the solution would cool down and eventually freeze. However, for this solar energy application, heat is available from the sunlight as infrared photons that are not being used by the semiconductor, so a continuous electrolysis at 1.35 volts is possible.*
[4] O. Khaselev and J. Turner, *Science* 1998, 285, 425.
[5] Kocha, S. S.; Turner, J. A.; Nozik, A. J. J. Electroanal. Chem. 1994, 367, 27.
[6] Kocha, S. S.; Turner, J. A. J. Electrochem. Soc. 1995, 142, 2625.

[7]   Kocha, S. S.; Turner, J. A. Electrochim. Acta 1996, 41, 1295.

[8]   Khaselev, O.; Turner, J. A. J. Electrochem. Soc. 1998, 145, 3335.

[9]   Allongue, P.; Blonkowski, S. J. Electroanal. Chem. 1991, 316, 57.

[10] Allongue, P.; Blonkowski, S.; Lincot, D. J. Electroanal. Chem. 1991, 300, 261.

[11] Yoneyama, H.; Sakamoto, H.; Tamura, H. Electrochim. Acta 1975, 20, 341.

[12] Nozik, A. J.; Memming, R. J. Phys. Chem. 1996, 100, 13061.

[13] Allongue, P.; Cachet, H.; Horowitz, G. J. Electrochem. Soc. 1983, 130, 2352.

[14] Allongue, P.; Cachet, H. J. Electrochem. Soc. 1984, 131, 2861.

[15] Watts, D. K.; Koval, C. A. J. Phys. Chem. 1996, 100, 5509.

[16] Uhlendorf, I.; Reineke-Koch, R.; Memming, R. Ber. Bunsenges. Phys. Chem. 1995, 99, 1082.

[17] Allongue, P.; Blonkowski, S.; Souteyrand, E. Electrochim. Acta 1992, 37, 781.

[18] Kelly, J. J.; Memming, R. J. Electrochem. Soc. 1982, 129, 730.

[19] Koval, C. A.; Segar, P. R. J. Am. chem. Soc. 1989, 111, 2004.

[20] Kobayashi, H.; Mizuno, F.; Nakato, Y. Jpn. J. Appl. Phys. 1994, 33, 6065.

[21] A preliminary analysis of impedance data using the series-parallel circuit between 40 Hz and 60 KHz indicated that the parallel resistor Rp was always greater than 30 Kohm. Moreover, Mott-Shottky (1/C2 vs. V) plots made with capacitances calculated using both the series-parallel and the series circuits gave similar trends in migration of flatband potentials with illumination. The Mott-Shottky plots were made using capacitance values in the region where the current was light limited and was invariant with applied potential. In this potential range, the Mott-schottky plots were also found to be linear. Deviations from linearity occurred in potential regions (closer to Vfb) where the current changed with potential and capacitnace data was not evaluated in this region.

[22] Uhlendorf, I.; Reineke-Koch, R.; Memming, R. J. Phys. Chem. 1996, 100, 4930.

[23] Tufts, B. J.; Abrahams, I. L.; Caley, C. E.; Lunt, S. R.; Miskelly, G.; Sailor, M. J.; Santangelo, P. G.; Lewis, N. S.; Hedman, B. M.; Roe, A. L.; Hodgson, K. O. J. Am. Chem. Soc. 1990, 112, 5123.

Table I.   Capacitance-Voltage and Current-Voltage measurements on untreated and metal treated p-GaInP$_2$ surfaces in 3M KOH solution.

	Vfb, dark	Vfb, light[a]	Vfb[b]	Voc, p[c]	Voc, n[c]
	V vs. SCE	V vs. SCE	V	V vs. SCE	V vs. SCE
Untreated	-0.19	-0.53	-0.34	-0.88	-0.52
Pt treated	-0.15	-0.39	-0.24	-0.67	-0.40
RuIII treated	-0.15	-0.24	-0.09	-0.67	-0.41
OsIII treated	-0.14	-0.44	-0.30	-0.88	-0.37
CoIII treated	-0.15	-0.38	-0.23	-0.77	-0.43
RhIII treated	-0.18	-0.26	-0.08	-0.64	-0.54

a. Vfb values measured at an illumination level corresponding to a current density of 0.7-1.0 mA/cm^2.
b. Band edge migration under illumination (Vfb, light - Vfb, dark)
c. Voc values observed for positive (p) and negative (n) going scans corresponding to a current density of 0.7-1.0 mA/cm^2.
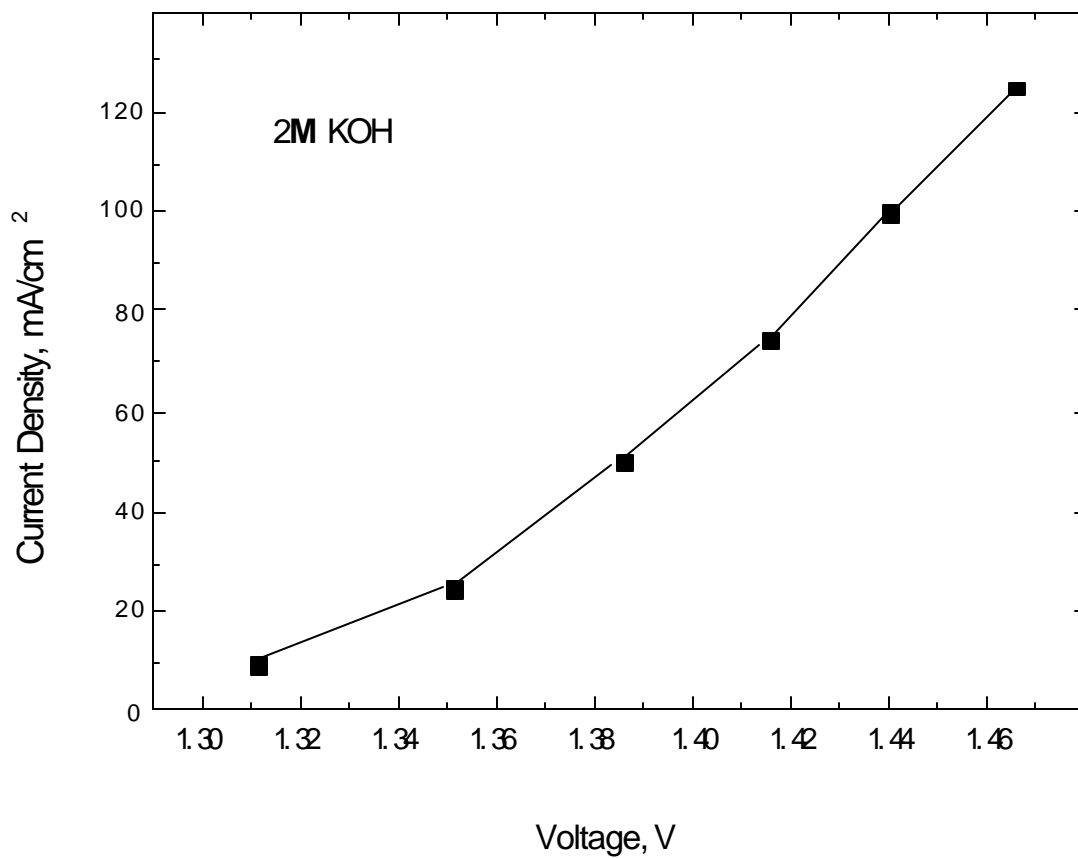
Figure 1. Current-voltage curve for water splitting in an electrochemical cell consisting of two Pt electrode mounted in the similar manner as in the PV/electrolysis system.
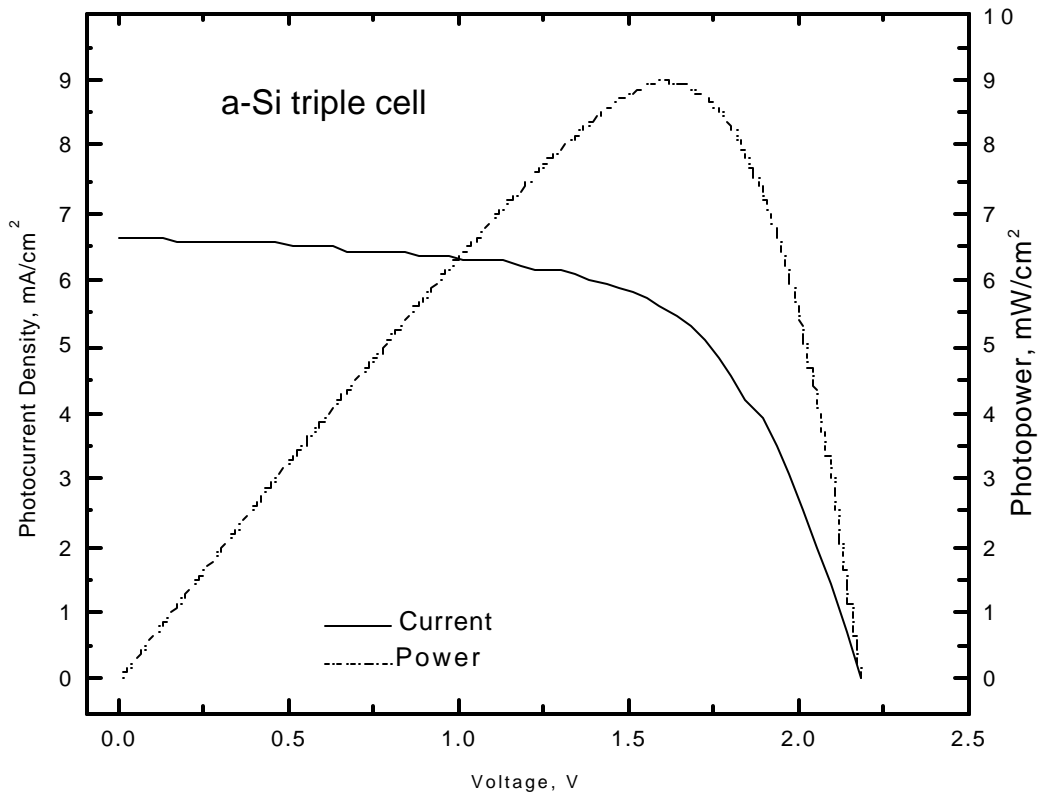
Figure 2. Measured indoor photocurrent and photopower/voltage characteristics for the triple p-i-n a-Si solar cell.
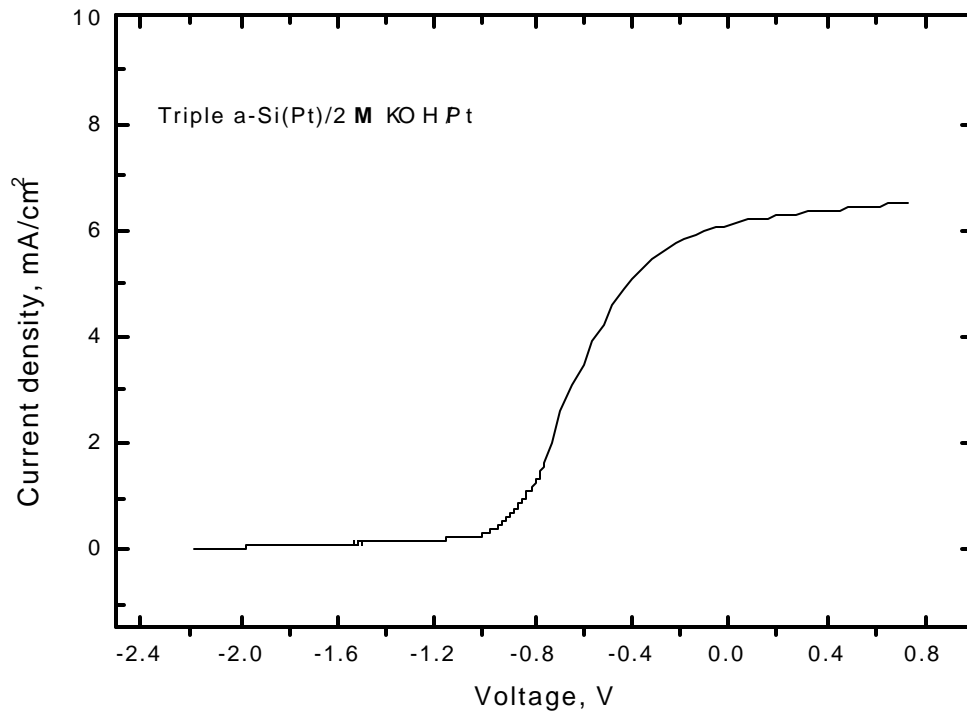
Figure 3. Measured indoor photocurrent/voltage characteristics of the triple p-i-n a-Si(Pt)/KOH/Pt PV/electrolysis solar cell.
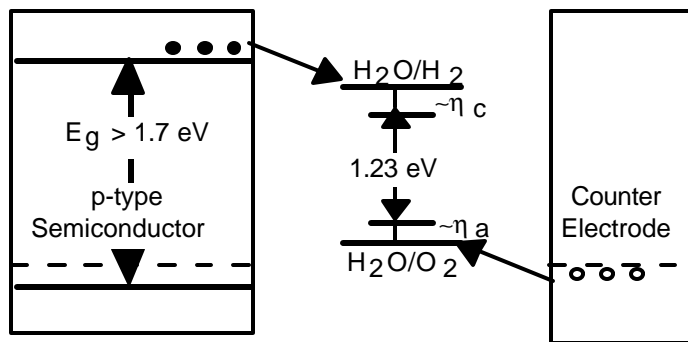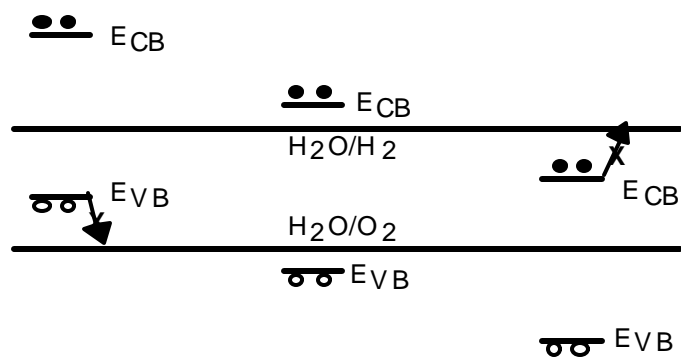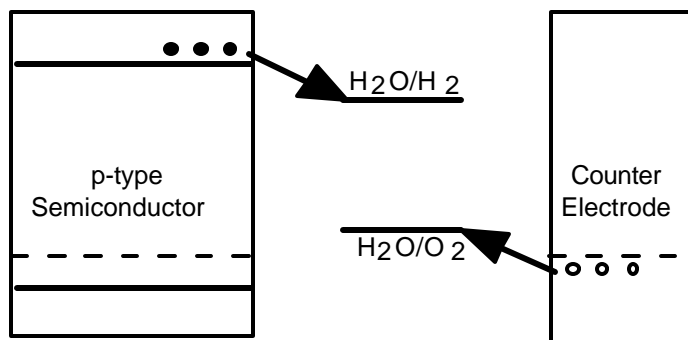
Figure 4. a) Bandgap criteria: The bandgap of the semiconductor must be greater than 1.7 eV. *a* and *c* indicate anodic and cathodic overpotentials for electrode reactions, respectively. b) Band Edge Overlap criteria: the band edges of the semiconductor must overlap the H2/H2O and O_2/H_2O redox potentials under H_2/O_2 evolution condition. c) Fast Kinetics criteria: Charge transfer across the semiconductor-liquid interface must be fast. For a successful hydrogen producing PEC system, all three criteria must be simultaneously satisfied.
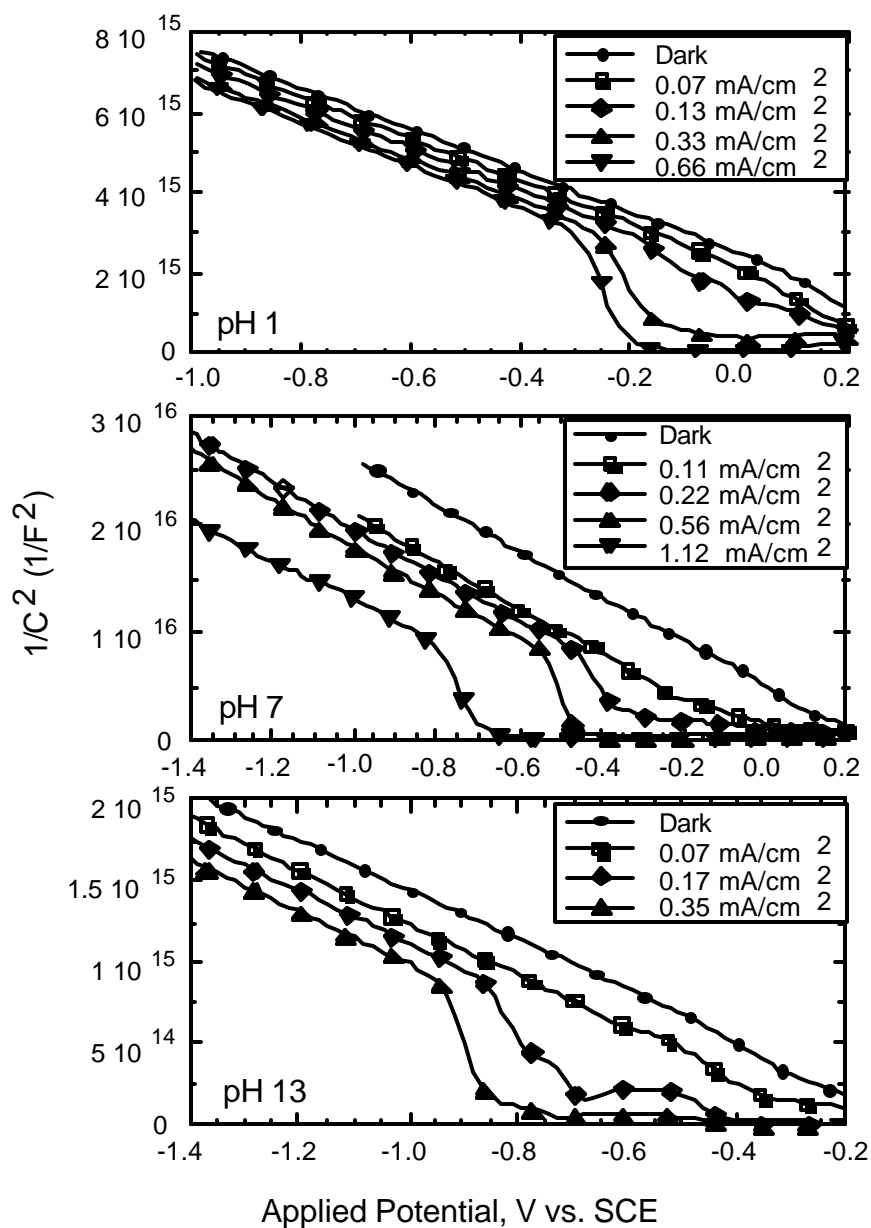
Figure 5. Mott-Schottky plots of p-GaInP$_2$ electrodes immersed in pH 1, 7 and 13, measured in the dark and under varying levels of illumination.
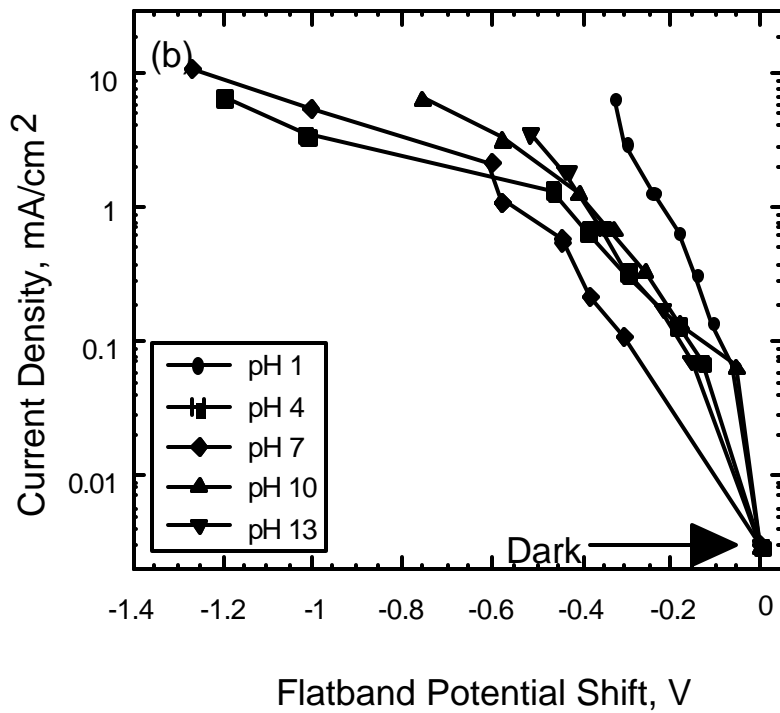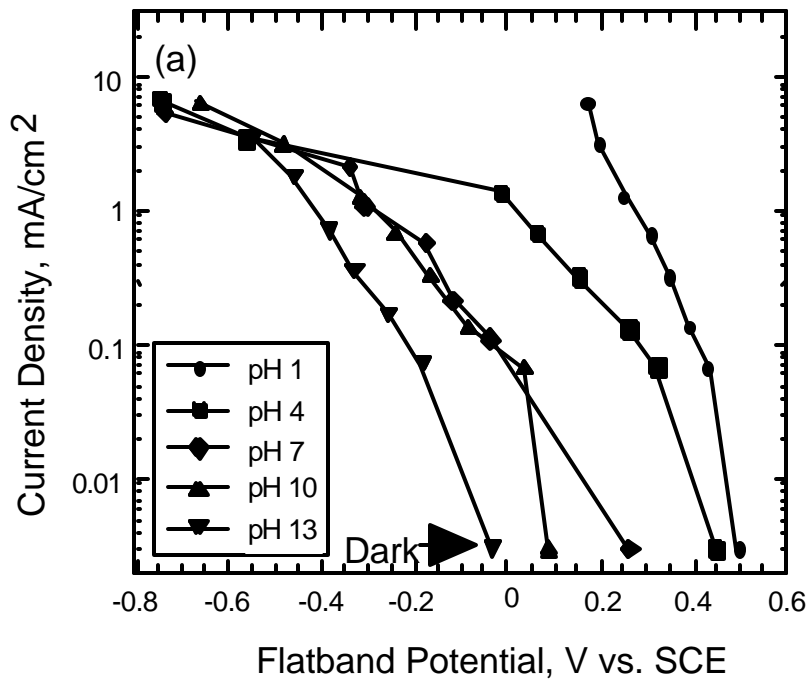
Figure 6. a) Flatband potentials of etched p-GaInP2 electrodes, measured vs. SCE, at five different pH values for varying levels of illumination. b) Migration of flatband potentials vs. the Vfb values observed in the dark (Vfb, light - Vfb, dark) in solutions of 5 different pH
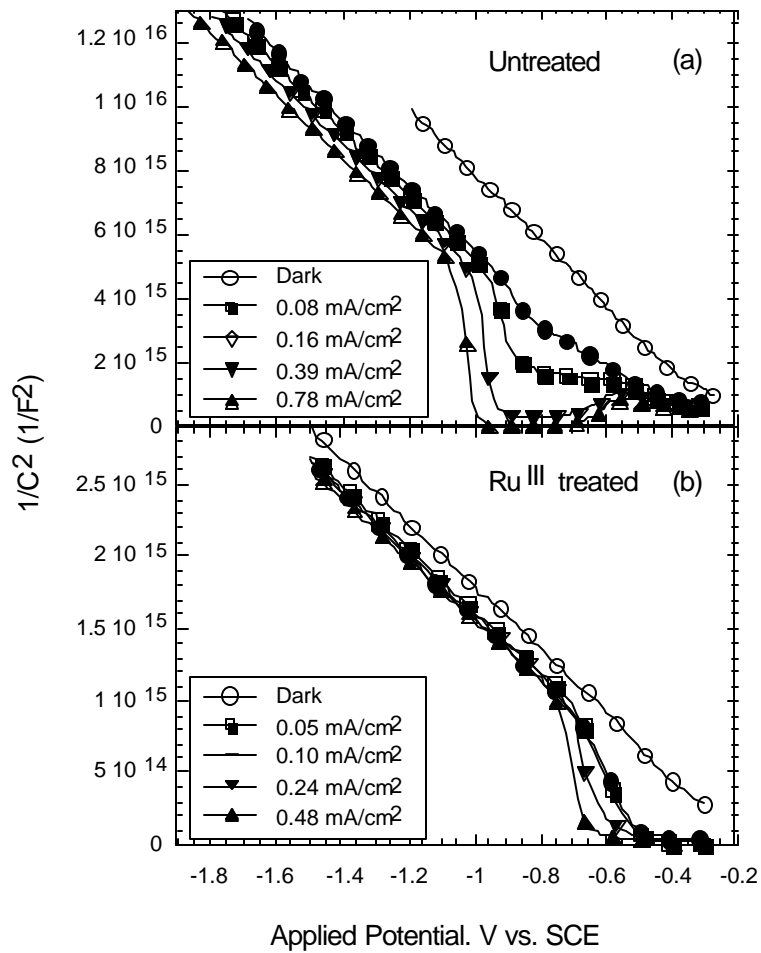
Figure 7. Mott-Schottky plots for a) an untreated and b) a RuIII-treated p-GaInP2 surface, measured in the dark and under illumination in 3 M KOH solution.
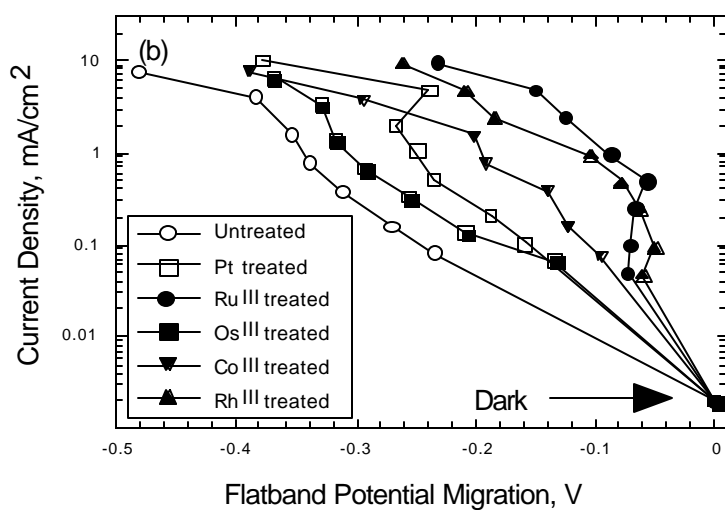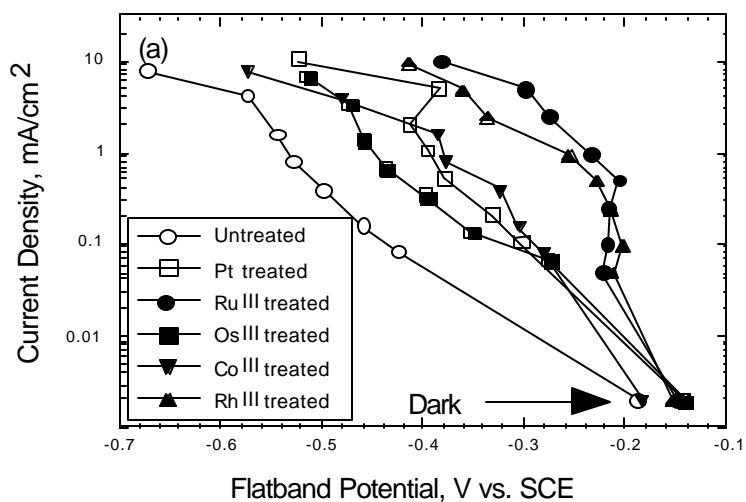
Figure 8. a) Flatband potentials of untreated (etched only) and metal-ion treated p-GaInP2 electrodes under illumination in the 3 M KOH solution. b) Migration of flatband potentials vs. the Vfb values observed in the dark (Vfb, light - Vfb, dark) in 3 M KOH solution.
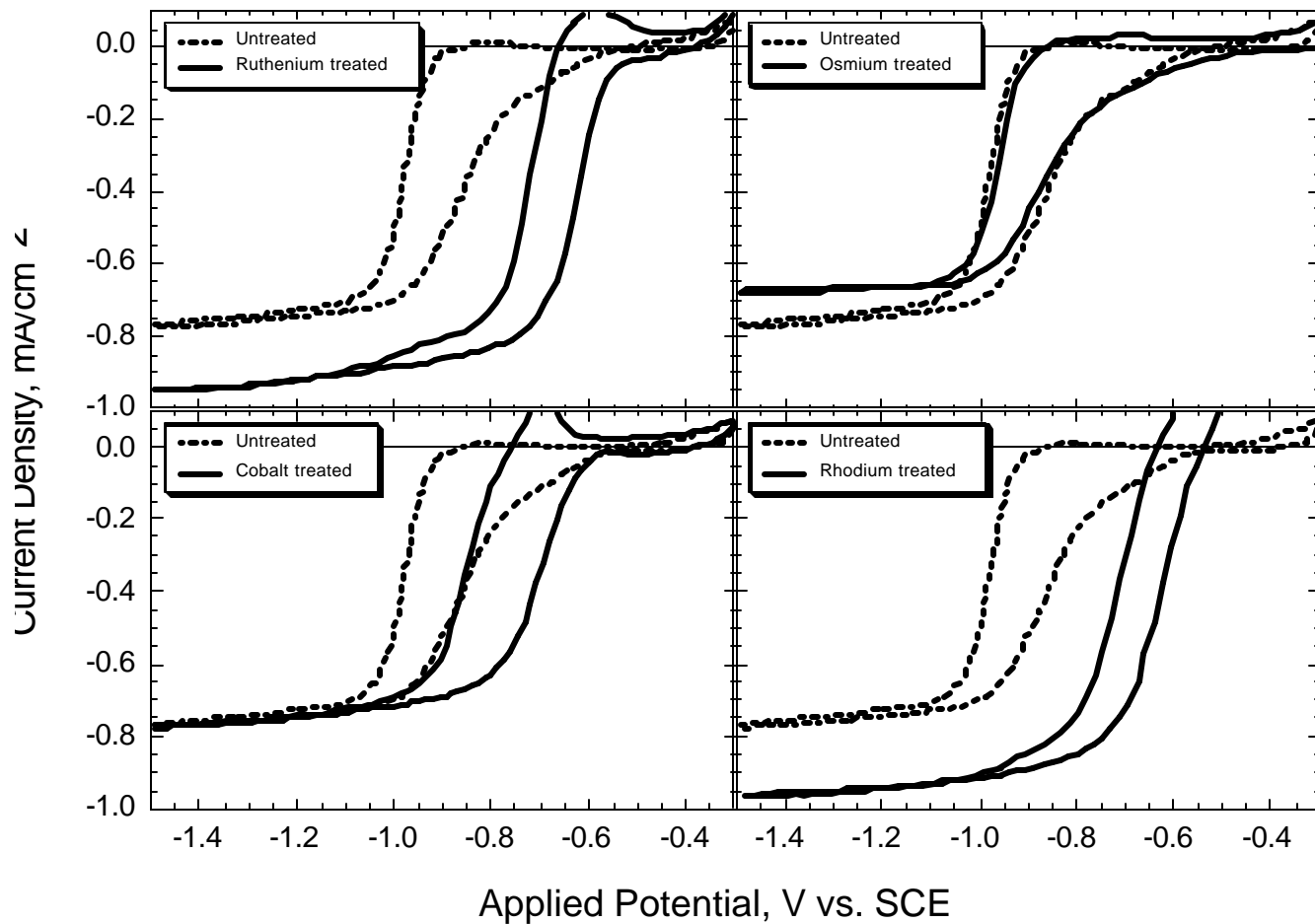
Figure 9. Current-Voltage (I-V) curves observed for untreated and metal-ion treated p-GaInP2 electrodes in 3 M KOH solution.